Received: 21 October 2020 | Revised: 30 December 2020 | Accepted: 13 January 2021
DOI: 10.22034/ecc.2021.256060.1112
Eurasian Chemical Communications
SAMI

FULL PAPER

Hydroxyapatite-gelatin and calcium carbonate-gelatin nanocomposite scaffolds: Production, physicochemical characterization and comparison of their bioactivity in simulated body fluid

Simin Sharifi[a] |Farzaneh Lotfipour[b,c] |Mohammad Ali Ghavimi[d] |Solmaz Maleki Dizaj[a,*] |Shahriar Shahi[a] |Javad Yazdani[d] |Masumeh Mokhtarpour[e] |Rovshan Khalilov[f,g,h]

[a]*Dental and Periodontal Research Center, Tabriz University of Medical Sciences, Tabriz, Iran*

[b]*Food & Drug Safety Research Center, Tabriz University of Medical Sciences, Tabriz, Iran*

[c]*Faculty of Pharmacy, Tabriz University of Medical Sciences, Tabriz, Iran*

[d]*Department of Oral and Maxillofacial Surgery, Faculty of Dentistry, Tabriz University of Medical Sciences, Tabriz, Iran*

[e]*Department of Physical Chemistry, University of Tabriz, Tabriz, Iran*

[f]*Department of Biophysics and Molecular Biology, Baku State University, Baku, Azerbaijan*

[g]*Institute of Radiation Problems, National Academy of Sciences of Azerbaijan, Baku, Azerbaijan*

[h]*International Research and Education Center of Nanobiotechnology and Functional Nanosystems, Drohobych Ukraine & Baku, Azerbaijan*

***Corresponding Author:**
Solmaz Maleki Dizaj
Email: maleki.s.89@gmail.com
Tel.: +98 9147351367

- Simin Sharifi and Farzaneh Lotfipour contributed equally.

In this study, HAP-gelatin and CC-gelatin nanocomposite scaffolds, as bioactive inorganic materials, were synthesized successfully through a chemical precipitation procedure. Next, characterization of the prepared nanocomposite scaffolds was completed using scanning electron microscopy (SEM), dynamic light scattering (DLS), zeta-sizer (for zeta potential measurement), X-ray diffraction (XRD) and Fourier transform infrared spectroscopy (FTIR). Then, we soaked the generated nanocomposite scaffolds in the simulated body fluid (SBF) for several times to investigate and compare the bioactivity of these nanocomposites and determine the percent of weight loss. The rate of calcium ions dissolution in SBF media was determined utilizing atomic absorption spectroscopy (AAS). The findings of characterization showed that the preparation of nanocomposites was successful with monodispersed nanosized particles, uniform agglomerated morphology, crystalline form, and negative surface charge. According to the results of the bioactivity test, both nanocomposite scaffolds were of high bioactivity, corroborated well with the patterns of calcium release. Calcium ions released from the HAP-gelatin nanocomposite were higher than that of the CC-gelatin. However, the bioactivity of CC was comparable with well-known bioactive HAP material. Therefore, it could be a promising alternative for use compared with HAP, the preparation of which is more complicated and expensive.

KEYWORDS

Hydroxyapatite; calcium carbonate; gelatin; nanocomposite scaffold; bioactivity; SBF.

Introduction

Bone related disorders are most significant problem in the modern orthopedic surgery due to improper life style, trauma and accidental injuries in early and middle age stages of life. Calcium phosphate-based ceramics are mostly used as orthopedic implant alternatives in the hard tissue regeneration due to their similar chemical composition, size, crystallinity and morphology to inorganic components of bone together their excellent biocompatibility [7]. Hydroxyapatite (HAP) is highly biocompatible, bioactive, and bio-resorbable.

Therefore, it is applicable for the repair of injured bone or tooth [9,39,47]. Calcium carbonate is known as a safe natural material [8,24,25]. Lately, it has been used for making microcapsules, nanotablets, composite films, and scaffolds [46].

Nanoparticles as ultrafine sub-micron particles may promote having materials, in comparison with their counterparts. Nanotechnology has shed new light on preparing low-priced systems by varying approaches [2,3,8,10,14,23-26,34,38,40]. Osteoconductive nanoparticles, such as HAP and CC can lead to a bond with the bone once applied to coat the bone and dental implants. Besides, possessing these materials may provide a suitable situation for creating new bone. These nanoparticles have more surface area resulting in higher reactivity. They can be used as exceptional structures in various arenas, particularly concerning the bone and dentistry domains [7,8,24,25,39,47].

Unfortunately, inorganic materials have poor mechanical strength in the aquatic environment. As a result, they cannot be applied for major load bearing. The seeding of the inorganic materials is controlled by organic materials through geometric, electrostatic, and stereochemical complementarities [7,15,37]. According to the literature, the biological reaction of inorganic nanoscaffolds can be further improved by combining the organic constituent materials, namely collagen, gelatin, and chitosan [32,35,36,50]. Biomimetic reports demonstrate that HAP and CC have been used to make structures with collagen as artificial bone alternates. However, collagen has some disadvantages such as the cost and problematic availability. Gelatin can be utilized as a cost effective substitute material. Furthermore, the immunogenicity and pathogen transmission issues of collagen are eliminated by gelatin [13].

In this study, HAP-gelatin and CC-gelatin nanocomposite scaffolds were synthesized successfully by chemical precipitation process. The synthesized nanocomposite scaffolds were then saturated in simulated body fluid (SBF) for several times to assess and compare their bioactivity. The designed simple preparation technique may be utilized to start and set up the easy and quick techniques for other nanocomposites with inorganic bases.

Materials

The used materials included commercial type, a bovine gelatin (Sigma-Aldrich, Germany). Sodium carbonate and calcium chloride were purchased from Merck Co. (Darmstadt, Germany), glycerin, calcium hydroxide, glacial acetic acid [CH3COOH] solution, orthophosphoric acid (Sigma-Aldrich, China), NaOH (0.1 M, Sigma-Aldrich, China).

Methods

The HA–gelatin nanocomposite scaffold was prepared by dissolving 0.35 g calcium hydroxide in diluted glacial acetic acid solution (2 mL). Then, 0.25 g of gelatin was poured to the media and allowed to stir at 55˚C for 3 hrs. In a separate flask, the orthophosphoric acid solution was prepared (0.2 M) in ammonia solution and a pH of 11.5. The prepared solutions were added slowly to the third beaker and continuous vigorous stirring was continued for 20 hrs. Then, the top solution was discarded. The precipitate was washed and centrifuged to obtain a HAP-gelatin nanocomposite scaffold. The powder was washed with distilled deionized water again and ultra-sounded. Finally it was freeze-dried to maintain its structure.

For the preparation of CC–gelatin nanocomposite scaffold, gelatin (15% w/w) was added into to 100 mL aqueous solution of $CaCl_2$ in the presence of glycerol at constant magnetic stirring (40 °C for 50 min) to gain a homogeneous solution. Then, the obtained solution was placed in an oven (37 ± 0.5 °C) for 5 h. The CC–gelatin nanocomposite scaffold as the dried powder was obtained finally.

Calcium carbonate and hydroxyl apatite materials without gelatin were also prepared in the same way without using gelatin.

Characterization

The mean nanocomposites size was found through the Dynamic Light Scattering (DLS) method (Malvern, United Kingdom) at 25 °C. In addition, the morphology of the nanocomposites was studied using SEM images (SEM, TESCAN, Warrendale, PA). Transmission electron microscopy (TEM) was used to confirm the presence of nanoparticles in the matrix of gelatin (JEM-2100F; JEOL, Tokyo, Japan). Zeta potential was assessed by a zeta-sizer (Malvern, UK) at 25 °C to obtain data concerning the surface charge of the nanocomposites. To do so, the fresh suspension was diluted with distilled water and injected into the capillary cell of the zeta-sizer. The X-ray diffraction (XRD) (Philips TW 1710) was applied to evaluate the crystallinity and phase determination information of the nanocomposites, in addition to pure CC and HAP materials. Data collection was performed at room temperature over the 2θ range of 20-70° with the scanning rate of 3˚/min. Moreover, the molecular structure and inter/intramolecular bonding of the synthesized nanocomposites were obtained through Fourier transform infrared spectroscopy (FTIR) (Thermo Nicolet-6700) in the range of 4000-400 cm^{-1}

Bioactivity test

The produced nano-powders were soaked in SBF (pH of 7.4 and 37 °C) over 28 days in order to assess their bioactivity (dissolution rate of calcium ions) [19,48]. Atomic absorption spectroscopy (AAS) was applied for this goal. The volume of SBF solution (in proportion to the surface area divided by 10) was poured on the samples [19].

Weight loss percent

The nanocomposites' weight loss was completed *in vitro* by samples incubation in SBF (pH: 7.4 and 37 °C) for 28 days. Afterwards, the specimens were dried at 50 °C for 24 hrs and the amounts for weight loss was calculated using the equation below:

Weight loss %= $(W_0-W_{28})/W_0$ *100

where W_0 refers to the initial weight of composites and W_{28} represents the weight at day 28.

Results

The mean size of the prepared materials is available in Figures 1 and 2. The results from DLS displayed a mean size of 13.84±0.91 nm (PDI of 0.23) for HAP-gelatin nanocomposites and 14.96±0.86 nm (PDA of 0.35) for CC-gelatin nanocomposites.

SEM and TEM results displayed uniform agglomerated morphology for both nanocomposite scaffolds (Figure 2). The presence of the nanoparticles in the gelatin matrix is also obvious according to TEM images. Zeta potential measurements (Figure 3) showed a negative surface charge for both nanocomposites (-27.80±0.34 mV for HAP-gelatin nanocomposites and -32.34±0.84 mV for CC-gelatin nanocomposites).

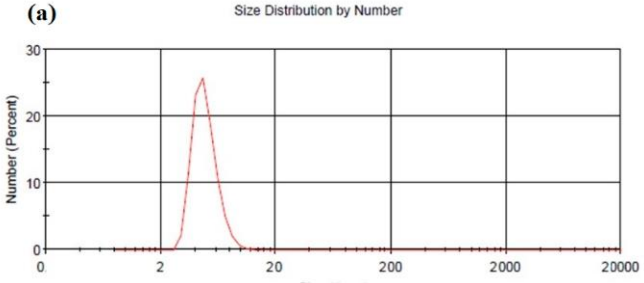

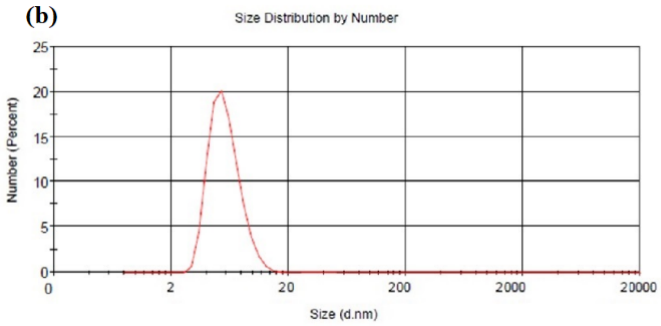

FIGURE 1 Size distribution of the HAP-gelatin nanocomposite (a) and CC-gelatin nanocomposite (b)

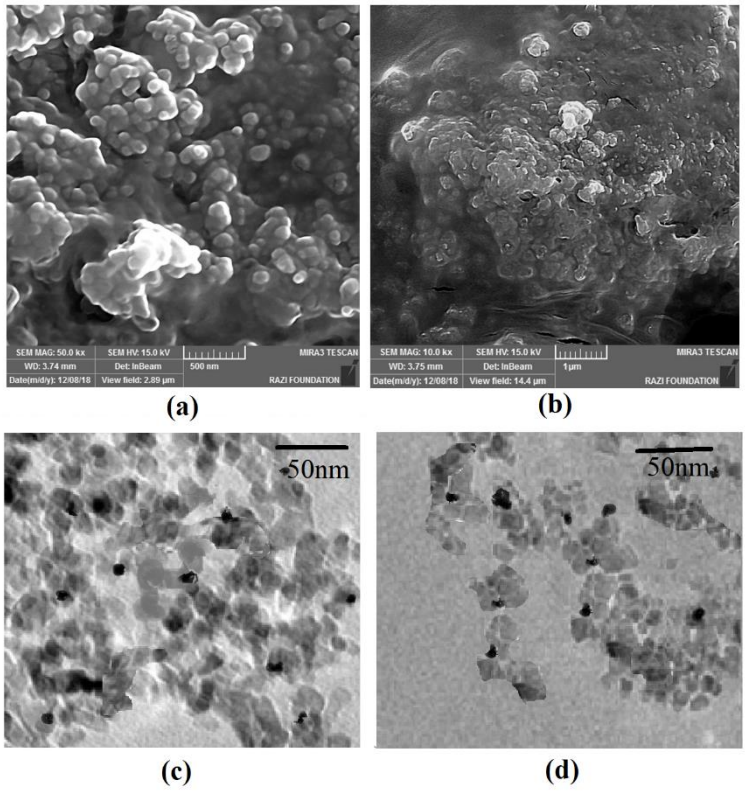

FIGURE 2 Microscopic images of the prepared nanocomposites: SEM image of the HAP-gelatin nanocomposite (a) and CC-gelatin nanocomposite (b), TEM image of the HAP-gelatin nanocomposite (c) and CC-gelatin nanocomposite (d)

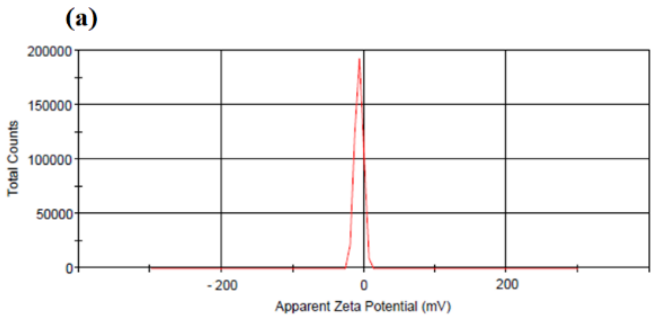

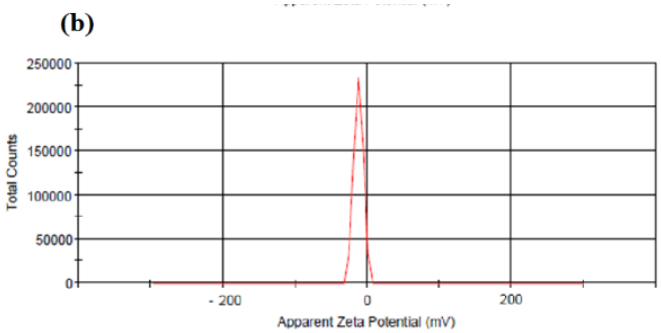

FIGURE 3 The amounts of zeta potential of the HAP-gelatin nanocomposite (a) and CC-gelatin nanocomposite (b)

The X-ray diffraction (XRD) patterns of the nanocomposites gives information about the degree of crystallinity. The results for the XRD outline showed the occurrence of sharp and high intensity patterns with no additional peaks (Figure 4). The XRD pattern of the samples can be completely indexed with the standard card (JCPDS file No.24-0033) for HAP and (JCPDS file No 47-1743) for CC. The peaks at 2θ of 26, 31.6, 32.92, 35.7, 40, 46.74, and 54.10° indicate the HAP [4, 42] peaks at 2θ of 29.4°, 39.4° and 56.5° shows that the composition of the $CaCO_3$ in nanocomposite is pure phase of calcite [30]. To assess the molecular structure of the synthesized HAP-gelatin nanocomposites, FT-IR was applied. Figure 5 shows FTIR results of the prepared nanocomposites. FT-IR peaks displayed all typical peaks of the nanocomposites with no additional peaks.

Figure 6 shows the releasing of calcium ions from nanocomposite scaffolds into SBF. More calcium ions were released from the HA-gelatin nanocomposite scaffold as compared with the CC-gelatin nanocomposite scaffold. The bioresorbability of the prepared nanocomposites is shown in Figure 7. The amount of calcium release from both nanocomposites agreed well with the calcium release outline of biological apatite [16,22].

Figure 8 displays the weight loss behavior of the prepared nanocomposites. The weight loss of the both nanocomposites showed a decreased curve compared with the pure CC and HAP materials (according to previous reports) [27,49].

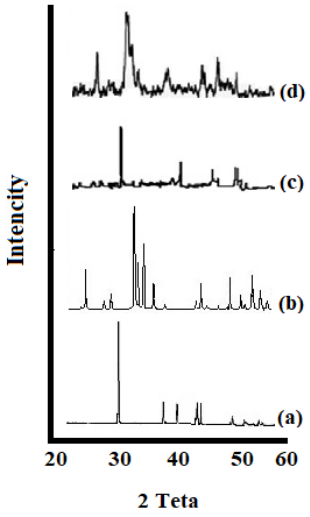

FIGURE 4 X-ray peaks for Calcium carbonate material (a), hydroxyl apatite material (b), CC-gelatin nanocomposites (c) and HAP-gelatin nanocomposites (d)

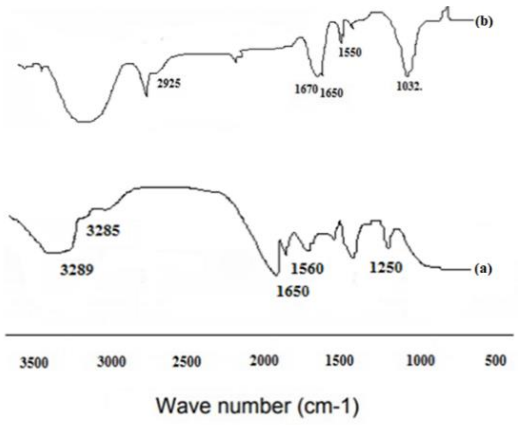

FIGURE 5 FT-IR spectra for CC-gelatin nanocomposites (a) and HAP-gelatin nanocomposites (b)

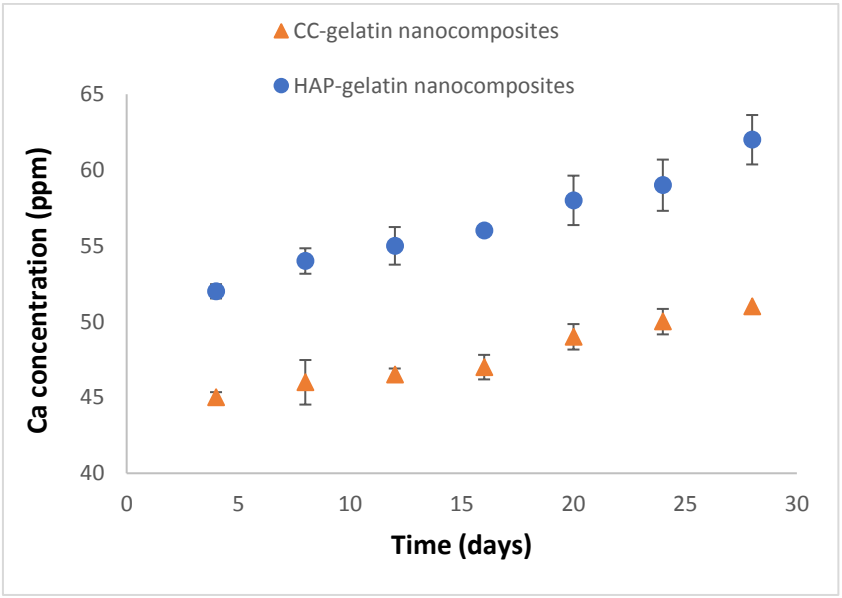

FIGURE 6 Release of calcium ions from the prepared nanocomposites

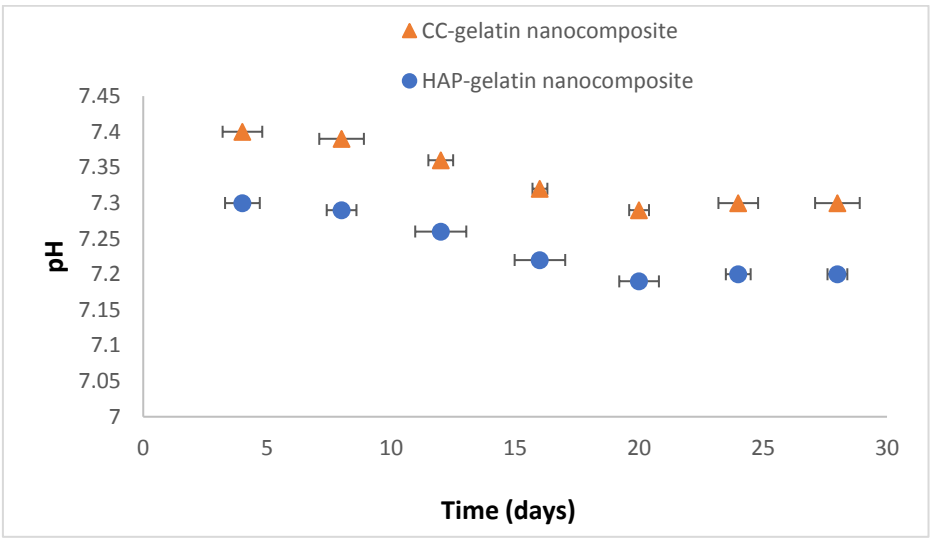

FIGURE 7 The pH changes of SBF solution versus time for prepared nanocomposites

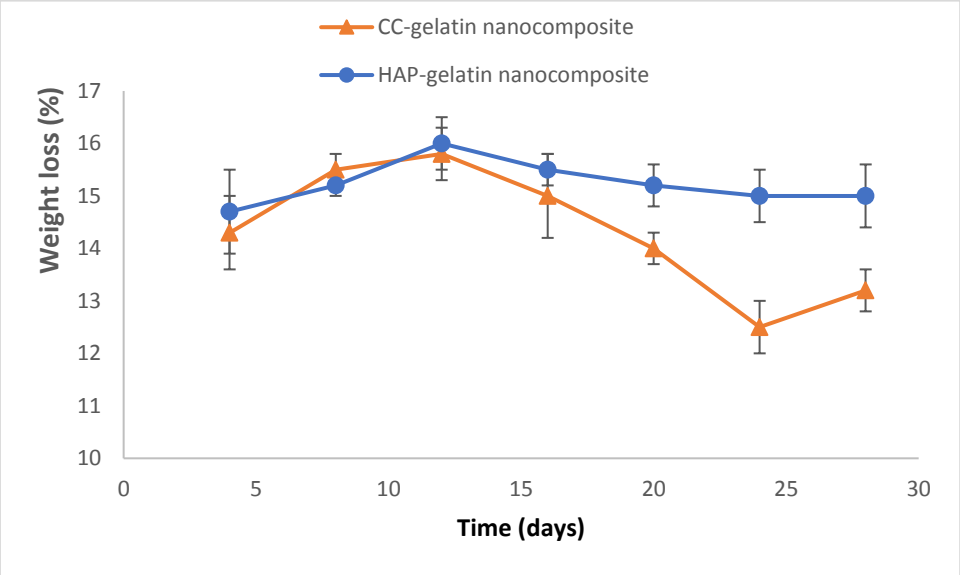

FIGURE 8 The weight loss percent versus time for the prepared nanocomposites

Discussion

Most types of the expanded scaffolds are not able to mimic the bone nanostructure [5,20]. Consequently, a scaffold with the capacity of mimicking the bone structure at the nano-scale level could be a favorable alternative to conventional bone grafts [6,18].

The biocompatibility and bioactivity possessions of HAP and CC nanoparticles have been outstanding concerning bone tissue engineering owing to their similarity with body hard tissues [11,44]. These nanoparticles can enhance the contact reaction and stability at the interface of artificial and natural bone [28]. The size of a particle is a remarkable variable for controlling the behavior of the HAP and CC powders in dental and orthopedic fields. The nanometer size of HAP and CC particles results in enhanced surface wettability improving vitronectin adsorption (osteoblast adhesion protein). In addition, the conformations might alter as a result of nanometer size improving osteoblast performance [45].

Precipitation procedure is an easy, quick, low cost and size-controllable method for synthesizing nanoparticles. The prepared nanocomposites in the current study indicated a particle size of narrow distribution (PDI values of 0.23 and 0.35). Some researchers believe that PDI values of 0.1–0.25 and over 0.5 show narrow and broad size distribution, respectively [8, 25]. As a result, the generated nanocomposites with PDI values of 0.23 for HAP-gelatin nanocomposites and 0.35 for CC-gelatin nanocomposites had a narrow size distribution. SEM images reveal aggregates with spherical and uniform morphology with a narrow size distribution confirming the findings of DLS examination.

The zeta potential for the colloidal particles plays a major part in determining their possessions. Zeta potential is one of the main factors commonly used for predicting suspension stability. Generally, an amount larger than ±60 mV indicates high stability, while a zeta potential lower than ±5 mV usually results in low stability. Zeta potential for the prepared nanocomposites was obtained as -27.80±0.34 mV for HAP-gelatin nanocomposites and -32.34±0.84 mV for CC-gelatin nanocomposites. Moreover, the reports have revealed that negative zeta potentials show a significantly promising influence on the attachment and proliferation of the osteoblasts. Based on these reports, a

negative zeta potential value might enhance the in vivo biological features. Consequently, the nanocomposites prepared in the present investigation may be superiorly attached to the bone cells [7,8,25,32].

The X-ray diffraction picks of the prepared nanocomposites were compared with the standard file showing a good match for the intensity and position of peaks. In addition, the X-ray diffraction picks could be utilized to calculate the percent of crystallinity in the structures by the XRD deconvolution technique, in which the amorphous and crystalline contributions to the diffraction spectrum were separated. The X-ray pattern of both nanocomposites demonstrated the dominance of the crystalline phase over the amorphous phase for both nanocomposites. It should be noted that the percent of crystallinity was higher for the CC-gelatin nanocomposite, compared with the HAP-gelatin nanocomposite. The crystallinity of both nanocomposites was lower than the pure HAP and CC, which could be attributed to the amorphous nature of gelatin [29].

According to Figure 5, the FT-IR spectrum of the generated nanocomposites indicated the numbers of all main bands. An amide I mode specified that HAP-gelatin composites had mostly an α-helical configuration, which was further confirmed by the appearance of amide II at ~1550 cm^{-1}. The hydroxyl group (-OH) of HAP was shown to have a stretching bond (4000-3300 cm^{-1}). The phosphate band was found at 1032 cm^{-1} [17]. The CC-gelatin composites had the amide I band showing C=O stretching/hydrogen bonding coupled with COO at the wavenumbers of 1650 cm^{-1}. Amide II that demonstrates the bending vibrations of N-H groups and stretching vibrations of C-N groups is at 1560 cm^{-1}. We obtained the vibrations of C-N and N-H groups of bound amide (amide-III) or vibrations of CH2 groups of glycerol in the gelatin matrix at the wavenumbers of 1250 cm^{-1}. Moreover, peaks at 3280–3290 cm^{-1} showed NH-stretching coupled with hydrogen bonding [43].

The findings indicated that both fabricated nanocomposites had high bioactivity in the SBF solution. Based on the results, the HAP-gelatin nanocomposite released more calcium ions than the CC-gelatin nanocomposite. The level of calcium release from both synthesized nanocomposites was verified well with the outline of the calcium release of biological apatite reported by other investigators [16, 22]. Calcium ions released from both prepared nanocomposite scaffolds into SBF was quantitatively estimated to support the *in vitro* bio-resorbability [33]. The structural and chemical compositions of the materials may greatly affect solubility. Then, the size of crystallite is a remarkable strategic variable for HAP and CC behavior in vitro. As a result, the engineering of the nano-crystallite size can stimulate the resorbability of HA.

Solubility of the materials determines the pH values. As a physicochemical rule, solubility increases with decreases in the pH [12]. Figure 7 shows that the bioresorbability rate of the HAP is higher than that of the CC. Furthermore, the obtained data suggest that CC should be classified as a bioactive material. Some reports presented that the new bone formation reaction of CC is similar to that of the bioactive hydroxyapatite [21, 31]. Ohgushi et al. reported that the interaction of osteogenic cells derived from porous brain cells and porous CC was confirmed without affecting existing host bone [31]. Besides, the chemical or surface alteration of gelatin can affect solubility rate significantly to provide slow biodegradation profile over several months *in vivo* [41].

The weight loss of both nanocomposites had a diminishing curve (Figure 8), compared with pure CC and HAP materials that proved that gelatin amount augmented the interaction between CC and HAP particles, leading to low degradation and high stability of the nanocomposites [1].

Conclusion

HAP-gelatin and CC-gelatin nanocomposite scaffolds were generated successfully by chemical precipitation procedure as an easy and rapid method. Both nanocomposite scaffolds were found to have high bioactivity, corroborated well with the pattern of the calcium release of biological amounts. HAP-gelatin nanocomposite released more calcium ions than the CC-gelatin nanocomposite. It could be concluded that the prepared nanocomposite scaffolds might be more beneficial for bone defects treatment, compared with conventional HAP. In addition, the close competitive bioactivity of CC with well-known bioactive HAP material is promising for the application of this available material instead of HAP, the preparation of which is more complicated and expensive. The designed simple preparation technique may be utilized to start and set up the easy and quick techniques for other nanocomposites with inorganic bases.

Acknowledgements

This study was based on a thesis entitled "Preparation of calcium carbonate-gelatin and hydroxy apatite-gelatin nanocomposite scaffolds, evaluation of their physicochemical properties, cytotoxicity and comparison of their bioactivity in SBF and artificial saliva" registered at Tabriz University of Medical Sciences (number; 61500). The Vice-Chancellor for Research at Tabriz University of Medical Sciences provided financial support for this research that is greatly acknowledged.

Orcid:

Simin Sharifi:
https://orcid.org/0000-0002-3020-3779
Farzaneh Lotfipour:
https://orcid.org/0000-0002-0774-9466
Mohammad Ali Ghavimi:
https://orcid.org/0000-0002-6638-2799
Solmaz Maleki Dizaj:
https://orcid.org/0000-0003-4759-7222
Shahriar Shahi:
https://orcid.org/0000-0003-4616-5145
Javad Yazdani:
https://orcid.org/0000-0002-5900-890X
Masumeh Mokhtarpour:
https://orcid.org/0000-0003-2906-5847
Rovshan Khalilov:
https://orcid.org/0000-0002-8684-1390

References

[1] M.H. Aghajan, M. Panahi-Sarmad, N. Alikarami, S. Shojaei, A. Saeidi, H.A. Khonakdar, M. Shahrousvan, V. Goodarzi, *Eur. Polym. J.*, **2020**, *131*, 109720.
[2] E. Ahmadian, S.M. Dizaj, E. Rahimpour, A. Hasanzadeh, A. Eftekhari, J. Halajzadeh, H. Ahmadian, *Mater. Sci. Eng. C*, **2018**, *93*, 465-471.
[3] E. Ahmadian, S.M. Dizaj, S. Sharifi, S. Shahi, R. Khalilov, A. Eftekhari, M. Hasanzadeh, *Trends Anal. Chem.*, **2019**, *116*, 167-176.
[4] N.H.A. Camargo, C. Soares, E. Gemelli, *Mater. Res.*, **2007**, *10*, 135-140.
[5] A.H. Dewi, I.D. Ana, J. Wolke, J. Jansen, *J. Biomed. Mater. Res. A*, **2013**, *101 A*, 2143-2150.
[6] A.H. Dewi, I.D. Ana, J. Wolke, J. Jansen, *J. Biomed. Mater. Res. A*, **2015**, *103*, 3273-3283.
[7] S.M. Dizaj, M. Mokhtarpour, H. Shekaari, S. Sharifi, *Journal of Advanced Chemical and Pharmaceutical Materials (JACPM)*, **2019**, *2*, 111-115.
[8] S.M. Dizaj, F. Lotfipour, M. Barzegar-Jalali, M.-H. Zarrintan, K. Adibkia, *J. Drug Deliv. Sci. Tec.*, **2016**, *35*, 16-23.
[9] S.M. Dizaj, A. Maleki, F. Lotfipour, S. Sharifi, F. Rezaie, M. Samiei, *Biointerface Res. Appl. Chem.*, **2018**, *8*, 3670-3673.
[10] A. Eftekhari, M. Hasanzadeh, S. Sharifi, S.M. Dizaj, R. Khalilov, E. Ahmadian, *Int. J. Biol. Macromol.*, **2018**, *117*, 993-1001.
[11] M. Fathi, A. Hanifi, *Mater. Lett.*, **2007**, *61*, 3978-3983.
[12] A. Göpferich, *Biomaterials*, **1996**, *17*, 103-114.
[13] S. Gorgieva, V. Kokol. Collagen- vs. Gelatine-Based Biomaterials and Their

Biocompatibility: Review and Perspectives. **2011**.
[14] E. Hamidi-Asl, J.-B. Raoof, N. Naghizadeh, S. Sharifi, M.S. Hejazi, *Journal of Chemical Sciences*, **2015**, *127*, 1607-1617.
[15] A. Hamidi, S. Sharifi, S. Davaran, S. Ghasemi, Y. Omidi, M.-R. Rashidi, *BioImpacts: BI*, **2012**, *2*, 97-103.
[16] A. Hanifi, M.H. Fathi, *Iran. J. Pharm. Sci.*,, **2008**, *4*, 141-148.
[17] M.J. Hossana, M. Gafurb, R. Kadirb, M.M. Karima, *International Journal of Engineering & Technology IJET-IJENS*, **2014**, *14*, 24-32.
[18] I.K. Januariyasa, I.D. Ana, Y. Yusuf, *Materials Science and Engineering C*, **2020**, *107*, 110347.
[19] T. Kokubo, H. Takadama, *Biomaterials*, **2006**, *27*, 2907-2915.
[20] S.C.G. Leeuwenburgh, I.D. Ana, J.A. Jansen, *Acta Biomaterialia*, **2010**, *6*, 836-844.
[21] A. Lemos, J. Ferreira, *Materials Science and Engineering: C*, **2000**, *11*, 35-40.
[22] D.-M. Liu, T. Troczynski, W.J. Tseng, *Biomaterials*, **2001**, *22*, 1721-1730.
[23] A. Maleki, A. Karimpour, M. Mokhtarpour, S.M. Dizaj, *Journal of Advanced Chemical and Pharmaceutical Materials (JACPM)*, **2018**, *1*, 73-76.
[24] S. Maleki Dizaj, M. Barzegar-Jalali, M.H. Zarrintan, K. Adibkia, F. Lotfipour, *Expert Opin. Drug Deliv.*, **2015**, *12*, 1649-1660.
[25] S. Maleki Dizaj, F. Lotfipour, M. Barzegar-Jalali, M.-H. Zarrintan, K. Adibkia, *Artificial Cells, Nanomedicine, and Biotechnology*, **2017**, *45*, 535-543.
[26] S. Maleki Dizaj, S. Sharifi, E. Ahmadian, A. Eftekhari, K. Adibkia, F. Lotfipour, *Expert Opin. Drug Deliv.*, **2019**, *16*, 331-345.
[27] K.R. Mohamed, H.H. Beherei, Z.M. El-Rashidy, *J. Adv. Res.*, **2014**, *5*, 201-208.
[28] R. Murugan, S. Ramakrishna, *J. Cryst. Growth.*, **2005**, *274*, 209-213.
[29] Z. Nabipour, M. Nourbakhsh, M. Baniasadi, *Nanomedicine Journal*, **2016**, *3*, 127-134.
[30] M. Ni, B.D. Ratner, *Surface and Interface Analysis: An International Journal Devoted to the Development and Application of Techniques for the Analysis of Surfaces, Interfaces and Thin Films*, **2008**, *40*, 1356-1361.
[31] H. Ohgushi, M. Okumura, S. Tamai, E.C. Shors, A.I. Caplan, *Journal of Biomedical Materials Research*, **1990**, *24*, 1563-1570.
[32] S. Ranganathan, K. Balagangadharan, N. Selvamurugan, *Int. J. Biol. Macromol.*, **2019**, *133*, 354-364.
[33] H. Ren, A. Li, B. Liu, Y. Dong, Y. Tian, D. Qiu, *Sci. Rep.*, **2017**, *7*, 3622.
[34] M. Saeedi, M. Eslamifar, K. Khezri, S.M. Dizaj, *Biomed. Pharmacother.*, **2019**, *111*, 666-675.
[35] S. Salatin, M. Jelvehgari, *Pharmaceutical Sciences*, **2017**, *23*, 84-94.
[36] S. Salatin, M. Alami-Milani, R. Daneshgar, M. Jelvehgari, *Drug Dev. Ind. Pharm.*, **2018**, *44*, 1613-1621.
[37] S. Salatin, J. Barar, M. Barzegar-Jalali, K. Adibkia, F. Kiafar, M. Jelvehgari, *Jundishapur Journal of Natural Pharmaceutical Products*, **2018**, *13*, e12873.
[38] S. Shahi, J. Yazdani, E. Ahmadian, S. Sunar, S.M. Dizaj, *Journal of Advanced Chemical and Pharmaceutical Materials (JACPM)*, **2018**, *1*, 62-64.
[39] S. Sharifi, M. Mokhtarpour, A. Jahangiri, S. Dehghanzadeh, S. Maleki-Dizaj, S. Shahi, *Biointer. Res. Appl. Chem.*, **2018**, *8*, 3695-3699.
[40] S. Sharifi, S.Z. Vahed, E. Ahmadian, S.M. Dizaj, A. Eftekhari, R. Khalilov, M. Ahmadi, E. Hamidi-Asl, M. Labib, *Biosens. Bioelectron.*, **2020**, *150*, 111933.
[41] Z. Sheikh, S. Najeeb, Z. Khurshid, V. Verma, H. Rashid, M. Glogauer, *Materials*, **2015**, *8*, 5744-5794.
[42] M. Sumathra, K.K. Sadasivuni, S.S. Kumar, M. Rajan, *ACS omega*, **2018**, *3*, 14620-14633.
[43] Y. Wang, A. Liu, R. Ye, X. Li, Y. Han, C. Liu, *Int. J. Food Prop.*, **2015**, *18*, 2442-2456.
[44] T.J. Webster, C. Ergun, R.H. Doremus, R.W. Siegel, R. Bizios, *Biomaterials*, **2000**, *21*, 1803-1810.
[45] G. Williamson, W. Hall, *Acta. Metall. Sinica.*, **1953**, *1*, 22-31.

[46] G. Xu, N. Yao, I.A. Aksay, J.T. Groves, *J. Am. Chem. Soc.*, **1998**, *120*, 11977-11985.
[47] J. Yazdani, E. Ahmadian, S. Sharifi, S. Shahi, S.M. Dizaj, *Biomed. Pharmacother.*, **2018**, *105*, 553-557.
[48] Y. Yu, Z. Bacsik, M. Edén, *Materials*, **2018**, *11*, 1690.
[49] P.A. Zapata, H. Palza, B. Díaz, A. Armijo, F. Sepúlveda, J.A. Ortiz, M. Paz Ramírez, C. Oyarzún, *Molecules (Basel, Switzerland)*, **2018**, *24*, 126.
[50] Y. Zhang, V.J. Reddy, S.Y. Wong, X. Li, B. Su, S. Ramakrishna, C.T. Lim, *Tissue Engineering Part A*, **2010**, *16*, 1949-1960.

How to cite this article: Simin Sharifi*, Farzaneh Lotfipour*, Mohammad Ali Ghavimi, Solmaz Maleki Dizaj*, Shahriar Shahi, Javad Yazdani, Masumeh Mokhtarpour, Rovshan Khalilov. Hydroxyapatite-Gelatin and calcium carbonate- gelatin nanocomposite scaffolds: Production, physicochemical characterization and comparison of their bioactivity in simulated body fluid**.** *Eurasian Chemical Communications*, 2021, 3(2), 70-80. **Link:** http://www.echemcom.com/article_122503.html